

Physical: Full-length

Comparison of TEM specimen preparation of perovskite thin films by tripod polishing and conventional ion milling

Espen Eberg¹, Åsmund F. Monsen², Thomas Tybell^{1,3},
Antonius T. J. van Helvoort² and Randi Holmestad^{2,*}

¹Department of Electronics and Telecommunications, ²Department of Physics and ³NTNU Nanolab, Norwegian University of Science and Technology, 7491 Trondheim, Norway

*To whom correspondence should be addressed. E-mail: randi.holmestad@ntnu.no

Abstract In this article, the effects of the transmission electron microscopy (TEM) specimen preparation techniques, such as ion milling and tripod polishing on perovskite oxides for high-resolution TEM investigation, are compared. Conventional and liquid nitrogen cooled ion milling induce a new domain orientation in thin films of SrRuO₃ and LaFeO₃ grown on (001)-oriented SrTiO₃ substrates. This is not observed in tripod-polished specimens. Different ion milling rates for thin films and substrates in cross-section specimens lead to artefacts in the interface region, degrading the specimen quality. This is illustrated by SrRuO₃ and PbTiO₃ thin films grown on (001)-oriented SrTiO₃. By applying tripod polishing and gentle low-angle, low-energy ion milling while cooling the sample, the effects from specimen preparation are reduced resulting in higher quality of the TEM study. In the process of making face-to-face cross-section specimens by tripod polishing, it is crucial that the glue layer attaching the slabs of material is very thin (<50 nm).

Keywords specimen preparation, tripod, perovskite, HRTEM

Received 17 June 2008, accepted 22 August 2008

Introduction

Complex oxides, and in particular perovskites, are a class of materials showing a number of interesting properties such as ferroelectricity, ferromagnetism, high- T_c superconductivity, gigantic magnetoresistance – or combinations of these [1]. In order to implement these materials into devices, an understanding of size and interface effects is needed [2,3]. Transmission electron microscopy (TEM) is a promising technique to characterize structural, physical and chemical properties at an atomic scale [4]. In high-resolution TEM (HRTEM) the quality of the TEM specimens becomes a limitation factor [5], and with the realization of aberration-corrected TEMs, this effect is more prominent. Thus, it is crucial that the preparation does not deteriorate the TEM study of the specimen.

The conventional Ar-ion milling scheme can leave an amorphous surface layer on the specimen with a thickness up to 10 nm [6]. Such alteration leads to degradation of the electron channelling along atom columns and hence a decreased contrast in atomic resolution scanning TEM (STEM) [7]. A promising approach is to apply tripod polishing in

the specimen preparation procedure [8]. This pure mechanical specimen preparation technique has previously been applied successfully to Si for imaging of single atoms using annular dark field STEM (see, for example Voyles *et al.* [9]). Also for III–V semiconductors, this technique has demonstrated to give superior specimen quality compared to Ar-ion-milled specimens [10]. For these semiconductors, the preparation technique has proven to give thin specimens uniform/linearly varying thickness and less surface roughness compared to Ar-ion-milled specimens, as well as being site specific. In this work, the effects of conventional Ar-ion milling and tripod polishing of perovskite thin films and the possibilities in applying these techniques to three perovskite thin film systems are investigated.

Experimental details

Thin film materials

In order to probe how the specimen preparation techniques affect the materials, three different perovskite thin film (10–50 nm) materials were used in this study: (i) PbTiO₃ (PTO),

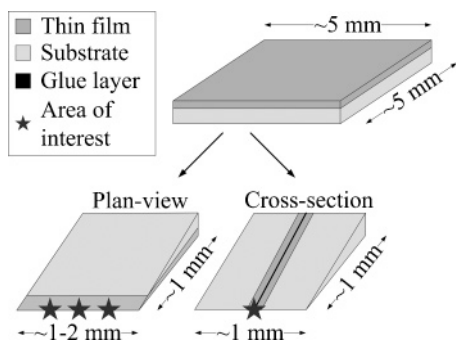


Fig. 1. Schematic diagram showing the geometry of plan-view and cross-section specimens prepared by tripod polishing. The areas of interest are highlighted with star(s). Note that the dimensions of film, substrate and glue layer thickness are not on scale.

(ii) SrRuO₃ (SRO) and (iii) LaFeO₃ (LFO). These materials represent different material classes within the perovskites, where PTO has a tetragonal phase and is ferroelectric with a critical temperature of 763 K [11], SRO has an orthorhombic phase and shows metallic behaviour [12] and LFO has an orthorhombic phase and is antiferromagnetic with a Néel temperature of 740 K [13].

All the thin films were grown on (001)-oriented cubic SrTiO₃ (STO) substrates by off-axis radio frequency magnetron sputtering [2]. Investigations by X-ray diffraction (XRD) and atomic force microscopy confirmed epitaxial growth of high crystalline quality. Domain structures were also examined by XRD.

Specimen preparation

Conventional ion-milled samples were prepared by mechanical grinding, followed by dimpling and Ar-ion milling in a *Gatan Precision Ion Polishing System* (PIPS). Acceleration voltages of 4–4.5 kV, incident beam angle of 4° and milling times of 1–2 h were typically used. Specimens with plan-view and cross-section geometries were prepared.

An *Allied Multiprep System* was used for tripod polishing of TEM specimens. The thin film samples were cut into slabs of $\sim 1 \times 1\text{--}2 \text{ mm}^2$. When cross-section specimens were made, two slabs were glued together with film sides facing each other using *Allied EpoxyBond 110*. The two slabs were clamped in order to provide a thin glue line and cured on a 100°C hot plate for about 1 h. Both plan-view and cross-section specimens were attached to a pyrex specimen holder using super glue and allowed to cure for at least 2 h. Cross-section specimens were attached with the interface normal to the pyrex surface, while plan-view specimens were attached with the film side facing the pyrex surface. The specimen geometries are illustrated in Fig. 1.

For the cross-section specimens, a reference plane was first polished, using diamond-lapping films (DLF). A 15- μm grain-size DLF was used to provide a planar surface. This was followed by 6-, 3-, 1-, 0.5- and 0.1- μm grain DLFs removing material equivalent to three times the grain size from

the previous step [14]. Additionally, scratches caused by debris had to be polished away. For the last three steps, *Allied GreenLube* was used as a lubricant and the specimen load reduced from 200 g to 50 g in order to avoid wedge chipping and scratches on the surface. As a final step, the reference plane was polished using a polyurethane cloth stained with a buffered silica solution with 20-nm particle size (*Allied Colloidal Silica Suspension*). Between every polishing step, the specimen was inspected for scratches and chipping of the edges under an optical microscope. Prior to polishing the other side, the specimen was lifted off the pyrex in an acetone bath and rinsed in ethanol.

For polishing of cross-section geometry, the scheme was the same as that for the plan-view geometry. The specimen was polished down to a thickness of 500 μm using a 15- μm DLF, where a wedge angle of 2° was introduced. The choice of wedge angle is a compromise between large electron transparent areas (low angle) and robust specimen (high angle) [14].

The specimens were polished down to 250-, 120- and 50- μm thickness using 15-, 6- and 3- μm DLFs, respectively. At 50- μm thickness the load was reduced from 200 g to no load and the specimens were polished with a 1- μm DLF and *GreenLube* lubricant until thickness fringes appeared, or the wedge started to chip off. Final polishing steps were done with 0.5- and 0.1- μm DLFs and 20-nm colloidal silica to further thin the wedge to electron transparency.

Specimens which were not tripod polished to electron transparency because of wedge chipping were thinned by low-energy, low-angle Ar-ion milling using a *Gatan Duo Ion Mill* while cooling the specimens to liquid nitrogen temperatures. Acceleration voltages of 3–3.5 kV, 8° incident angle and an initial milling time of 5 min were used. This was followed by additional 5 min at 2–2.5 kV acceleration voltage and 8° incident angle. If the specimen was not sufficiently thinned, the milling procedure was repeated once.

Characterization

For characterization of the specimens, two different TEMs, a *JEOL 2010F* equipped with a *Gatan 1K CCD camera* and a *Philips LaB₆ CM30* using negatives, both operating at 200 kV acceleration voltage, were used. Prior to investigations, the specimens were usually plasma cleaned in a *Fischione 1020 Plasma Cleaner* for 5 min.

Results and discussion

In Fig. 2a, a STO substrate plan-view specimen prepared by Ar-ion milling in a PIPS is shown [the specimen was mechanically thinned using a tripod polisher down to a thickness of 5–10 μm (similar thickness as grinded and dimpled specimens)]. Compared to the solely tripod-polished PTO thin film plan-view specimen in Fig. 2b, several specimen preparation effects can be seen. The amount of amorphous material at the wedge, marked with arrows in

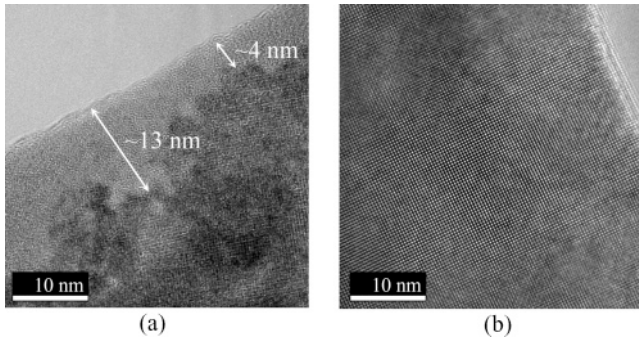


Fig. 2. Comparison of tripod polished and ion-milled specimens. (a) HRTEM micrograph of an ion-milled STO substrate (plan-view) specimen. The width of the amorphous surface extends over the crystalline part and is marked with arrows, spanning from ~ 4 to ~ 13 nm. (b) HRTEM micrograph of a tripod polished PTO/STO thin film plan-view specimen, showing a little change in phase contrast and no amorphous surface layer.

micrograph (a), of the ion-milled specimen is significant compared to the tripod-polished specimen. This is a permanently damaged surface layer that decreases the feature contrast in the micrographs. It is not possible to remove this layer using the plasma cleaner. The ion-milled sample also suffers from thickness variations and surface roughness that manifests as thickness and phase contrast variations. On the other hand, in the tripod-polished specimen, there are large areas of constant thickness showing phase contrast.

The surface roughness seen in Fig. 2a gives phase contrast problems which make interpretation of the micrograph difficult [15]. In Fig. 2a, this is demonstrated by a change of intensity in the lattice for different positions within the ion-milled specimen. In the tripod-polished specimen in Fig. 2b, there are much less phase contrast variations which make it easier to simulate and interpret the atomic features.

The micrograph in Fig. 2b shows that the wedge is thinned to electron transparency over large areas. With a 2° wedge angle, the total electron transparent area is estimated to be $100 \text{ nm} \times 2 \text{ mm}$, although the whole wedge is not suitable for HRTEM.

In Fig. 3 micrographs of a plan-view Ar-ion-milled (a) and a tripod-polished specimen (b) from a LFO thin film sample are shown. Selected area diffraction (SAD) patterns are shown for the ion-milled and tripod-polished specimens in Fig. 3c and d, respectively. The ion-milled specimen shows a third domain orientation, marked Z in the SAD pattern of the ion-milled specimen, compared to the tripod-polished specimen. Careful investigation by XRD showed that no Z-domains were present prior to TEM specimen preparation. These Z-domains have epitaxial relationships $[001]_{\text{LFO}} \parallel [001]_{\text{STO}}$ and $[100]_{\text{LFO}} \parallel [110]_{\text{STO}}$ which give a larger mismatch (0.69%) compared to the expected domain orientations $[001]_{\text{LFO}} \parallel [100]_{\text{STO}}$ and $[110]_{\text{LFO}} \parallel [001]_{\text{STO}}$ or $[001]_{\text{LFO}} \parallel [010]_{\text{STO}}$ and $[110]_{\text{LFO}} \parallel [001]_{\text{STO}}$ with the lowest mismatch (0.56%) calculated with bulk lattice parameters given by Seo *et al.* [13]. These observations agree with Barber [16]

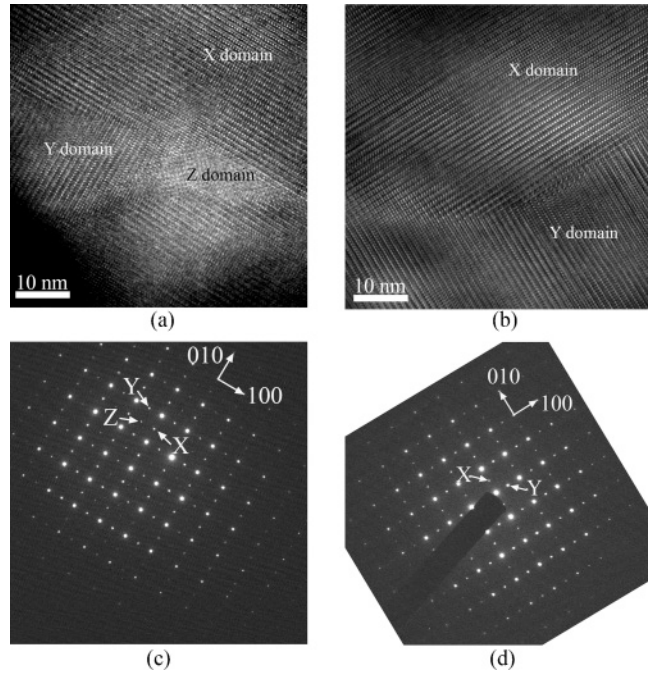


Fig. 3. Comparison of tripod polished and ion-milled plan-view specimens of LFO/STO thin films. (a) HRTEM micrograph of an ion-milled LFO/STO thin film plan-view specimen. The different domains are marked X, Y and Z according to domain orientation. (b) HRTEM micrograph of a tripod polished LFO/STO thin film plan-view specimen. The different domains are marked X and Y according to domain orientation. (c) SAD pattern from the ion-milled LFO/STO thin film plan-view specimen. Reflections identifying the domains are marked X, Y and Z. (d) SAD pattern from the tripod polished LFO/STO thin film plan-view specimen. Reflections identifying the domains are marked X and Y.

who has found that ion milling in addition to introducing an amorphous surface layer, also potentially can alter the crystal structure of the sample, caused by the heating during ion milling in various material systems.

For SRO thin films grown on STO, which have the same growth relation as LFO, we have found that Z-domains are present only in ion-milled TEM specimens. This has been confirmed by Pan *et al.* [17]. Hence, in order to study the domain structure for these orthorhombic perovskite thin film specimens, ion milling should be avoided.

For cross-section geometries the issue with different milling rate for different species can be a problem. In Fig. 4a, a cross-section specimen of a SRO thin film is shown. The different milling rate of SRO compared to STO is clearly visible. The interface region is completely milled away in the thinnest part of the sample leaving an amorphous layer. This effect can be explained by the combination of two different mechanisms described in the literature: (i) there are different milling rates caused by charging effects in the material. Undoped STO is an insulator and so more charge will build up and deflect incoming Ar^+ ions compared to what happens in the metallic conductive SRO. SRO is milled away faster than STO and will get more damage in the

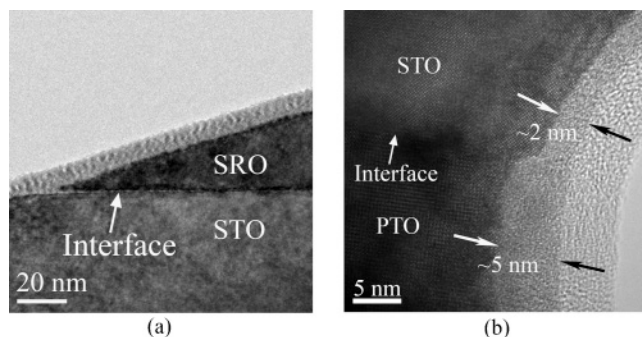


Fig. 4. Illustration of different milling rates for the thin film and substrate, respectively. (a) HRTEM micrograph of an ion-milled SRO/STO thin film cross-section specimen. The thin film is milled at different rates than the substrate, which results in a damaged region along the interface in the thinnest part of the specimen (see arrow). (b) HRTEM micrograph of a tripod polished and nitrogen cooled ion-milled PTO/STO thin film cross-section specimen. The width of the amorphous surface extending over the crystalline part is marked with arrows.

interface region caused by surface heating effects, since the very thin region will only consist of the surface layer [16]. (ii) Zandbergen *et al.* have suggested that this effect appears when ion-milled amorphous material fills up microcracks or protrusions caused by stress from ion milling [18]. In order to decrease surface roughness and preferential milling at the interface region, the milling time must be reduced without increasing the Ar-ion potential [19].

In Fig. 4b, a tripod-polished and low-angle, low-energy nitrogen cooled Ar-ion-milled PTO thin film cross-section specimen is shown. As for the SRO thin film in Fig. 4a, the PTO thin film is milled at a different rate than the STO substrate, but there is no damage in the interface region, allowing for investigation of this particular part of the specimen. Since the effect is more prominent for a specimen with larger difference in conductivity between thin film and substrate, mechanism (i) is probably the most important.

Short milling time, low angle and nitrogen cooling of the specimen result in a specimen with less surface roughness and a thinner damaged amorphous surface layer compared to ion milling at room temperature. This can be seen by comparing the width of the amorphous wedge which extends outside the crystalline area of the specimen. In Fig. 2b (tripod plan view), there is no apparent damage in the surface layer for STO, in Fig. 2a, there is a varying width spanning from ~ 4 to ~ 13 nm, while in Fig. 4b, the width is 2 nm for STO and 5 nm for PTO. Note that the amorphous surface layer is different from the carbonaceous contamination layer at the edge of the specimen. This layer was removed by 5 min of plasma cleaning, and no influence on the perovskite thin films was observed by (HR)TEM with this treatment.

It would be feasible to use only tripod polishing in specimen preparation and totally avoid ion milling. For plan-view specimens this is possible because the wedge is homogeneous in the lateral direction and will thus be polished

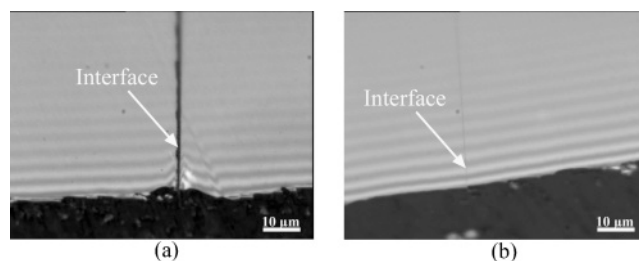


Fig. 5. Optical micrographs comparing tripod polished specimens with thin versus thick glue line. (a) 600 nm glue line: the thickness fringes bend outwards and become more narrow, indicating an increase in the thickness at the wedge. (b) <50 nm glue line: there is no change in the width of thickness fringes and no bending of the wedge, indicating a smooth interface region.

evenly. However, the wedge in cross-section specimens consists of at least one thin film/substrate interface and a glue layer. The difference in material properties across the interface causes the rate of polishing to be different along the wedge. This is illustrated in Fig. 5a and b where optical micrographs of two tripod-polished cross-section specimens are shown. In Fig. 5a, the optical interference fringes bend outwards indicating that the wedge is thicker in this area. This is caused by preferential polishing in the glue/specimen interface and is prominent for brittle materials as perovskite oxides. Another unwanted effect of this preferential polishing is that the crystal is bent and thus the zone axis varies with position in the specimen.

In Fig. 5b, a specimen with a very thin glue layer, below the optical resolution limit, is shown. The preferential polishing effect is significantly decreased and the thickness fringes extend parallel to the wedge across the interface. This indicates that the wedge is evenly thin and that the surface normal does not change as a function of position. Inspection of this specimen in TEM confirmed this. We have found that if the interface glue line is approximately <50 nm for thin film perovskite specimens, preferential polishing can be neglected. A similar conclusion has been drawn by Voyles, Grazul and Muller [14] who found a critical glue layer thickness of 100 nm for Si.

Conclusions

Ion milling can have a detrimental effect on the specimen and the resulting quality of the TEM studies. The ion-milled specimens have a permanently damaged, amorphous surface layer that is not visible in the tripod-polished specimens. For LFO and SRO thin films grown on STO substrates, an altered crystal structure was found for the ion-milled specimens compared to the tripod-polished specimens. Cross-section specimens were shown to suffer from different polishing rates creating artefacts at the interface between the thin film and the substrate in both PTO and SRO thin films grown on STO substrates.

For plan-view specimens, ion milling can be avoided by the use of pure mechanical tripod polishing. This is more

challenging for cross-section specimens because the non-uniformity of the wedge causes preferential polishing. This effect is minimized with an as thin as possible glue line and is negligible for glue line thicknesses <50 nm. In order to prepare cross-section specimens, specimen cooled gentle ion milling for a short period of time was applied in addition to tripod polishing.

Funding

Research Council of Norway (140553/420 for 'Micro- and Nano-based Materials Development', 158518/431 for 'Oxides for Future Information and Communication Technology' and 162874/V00 to E.E. and T.T.).

Acknowledgements

We would like to thank Bjørn. G. Soleim and Lena C. Wennberg for their work on specimen preparation, Prof. Jostein Grepstad and Tom Kristiansen for providing LFO thin films, Øystein Dahl for providing SRO thin films and Dr. Ryota Takahashi for providing PTO thin films.

References

- Ahn C, Triscone J-M, and Mannhart J. (2003) Electric field effect in correlated oxide systems. *Nature* **424**: 1015–1018.
- van Helvoort A, Dahl O, Soleim B, Holmestad R, and Tybell T. (2005) Imaging of out-of-plane interfacial strain in epitaxial $\text{PbTiO}_3/\text{SrTiO}_3$ thin films. *Appl. Phys. Lett.* **86**: 092907.
- Nakagawa N, Hwang H, and Muller D. (2006) Why some interfaces cannot be sharp. *Nat. Mater.* **5**: 204–209.
- Muller D, Nakagawa N, Ohtomo A, Grazul J, and Hwang H. (2004) Atomic-scale imaging of nanoengineered oxygen vacancy profiles in SrTiO_3 . *Nature* **430**: 657–661.
- Diebold A, Foran B, Kisielowski C, Muller D, Pennycook S, Principe E, and Stemmer S. (2003) Thin dielectric film thickness determination by advanced transmission electron microscopy. *Microsc. Microanal.* **9**: 493–508.
- McCaffrey J, Phaneuf M, and Madsen L. (2001) Surface damage formation during ion-beam thinning of samples for transmission electron microscopy. *Ultramicroscopy* **87**: 97–104.
- Mkhoyan K, Maccagnano-Zacher S, Kirkland E, and Silcox J. (2008) Effects of amorphous layers on ADF-STEM imaging. *Ultramicroscopy* **8**: 718–726.
- Klepeis S, Benedict J, and Anderson R. (1988) A grinding/polishing tool for TEM sample preparation. *MRS Symp. Proc.* **115**: 179–184.
- Voyles P, Muller D, Grazul J, Citrin P, and Gossmann H-J. (2002) Atomic-scale imaging of individual dopant atoms and clusters in highly n-type bulk Si. *Nature* **416**: 826–829.
- Okuno H, Takeguchi M, Mitsuishi K, Guo X, and Furuya K. (2008) Sample preparation of GaN-based materials on a sapphire substrate for STEM analysis. *J. Electron Microsc.* **57**: 1–5.
- Lines M and Glass A. (2001) *Principles and Applications of Ferroelectrics and Related Materials* (Oxford University Press, Oxford).
- Eom C, van Dover R, Phillips J, Werder D, Marshall J, Chen C, Cava R, and Fleming R. (1993) Fabrication and properties of epitaxial ferroelectric heterostructures with (SrRuO_3) isotropic metallic oxide electrodes. *Appl. Phys. Lett.* **63**: 2570–2572.
- Seo J, Dieker C, Fompeyrine J, Siegwart H, and Locquet J-P. (2006) Structural domains in antiferromagnetic LaFeO_3 thin films. *Int. J. Mater. Res.* **97**: 943–947.
- Voyles P, Grazul J, and Muller D. (2003) Imaging of individual atoms inside crystals with ADF-STEM. *Ultramicroscopy* **96**: 251–273.
- Karlik M. (2001) Lattice imaging in transmission electron microscopy. *Mater. Struct.* **8**: 3–15.
- Barber D. (1992) Radiation damage in ion-milled specimens: characteristics, effects and methods of damage limitation. *Ultramicroscopy* **52**: 101–125.
- Pan X, Jiang J, Tian W, Gan Q, Rao R, and Eom C. (1999) Effects of stress relaxation of epitaxial SrRuO_3 thin film on microstructures. *J. Appl. Phys.* **86**(8): 4188–4192.
- Zandbergen H, Hetherington C, and Gronsky R. (1988) Sample preparation of $\text{YBa}_2\text{Cu}_3\text{O}_{7-\delta}$ for high-resolution electron microscopy. *J. Supercond.* **1**: 21–34.
- Ayache J and Albarède P. (1995) Application of the ionless tripod polisher to the preparation of YBCO superconducting multilayer and bulk ceramics thin films. *Ultramicroscopy* **60**: 195–206.